JUDD-OFELT INTENSITY PARAMETERS OF ERBIUM DOPED LEAD TELLURITE GLASS

E. S. SAZALI, R. SAHAR*, S. K. GHOSHAL, S. ROHANI, R. ARIFIN
Advanced Optical Materials Research Group, Department of Physics, Faculty of Science, Universiti Teknologi Malaysia, Johor, Malaysia

Modification in the absorption characteristics of rare earth (RE) doped tellurite glasses is ever-demanding in photonics. Erbium (Er^{3+}) doped glasses with composition (80-x)TeO_2-15PbO-5$PbCl_2$-xEr_2O_3, where x=0.5, 1.0 and 1.5 mol% are synthesized using melt-quenching method and characterized via XRD and UV-Vis spectroscopy. The effects of varying Er_2O_3 concentration on the absorption spectral features of these glasses are examined. Judd-Ofelt (J-O) spectral analyses are carried out to determine the local structure and bonding in the vicinity of RE ions. XRD spectra confirm the amorphous nature of all the glass samples. UV-Vis-NIR spectra reveal seven prominent absorption peaks centered at 490, 526, 551, 652, 800, 982 and 1520 nm corresponding to the transitions from the ground state to various excited states of Er^{3+} ion. The experimental oscillator strengths calculated from the absorption spectra are used to evaluate three phenomenological J-O intensity parameters Ω_λ (λ=2, 4 and 6). The increase in glass density, refractive index and the values of Ω_4 and Ω_6 with the increase of RE concentration is ascribed to the change in glass network structures. The value of Ω_2 is first increased and then decreased at 1.5 mol% of erbium. Considerably higher value of branching ratio about 90% evidenced for $^4I_{9/2} \rightarrow {}^4I_{15/2}$ and $^4S_{3/2} \rightarrow {}^4I_{15/2}$ transitions imply that strong green and red emissions are attainable from such samples. The highest value of τ_{rad} is observed to be 1.02 ms for the glass with 0.5 mol% of Er_2O_3.Our findings may be useful for the development of functional glasses.

(Received May 28, 2014; Accepted October 27, 2014)

Keywords: Tellurite glass; Rare-earth; Oscillator strength; Absorbance; Judd-Ofelt.

1. Introduction

The observation of large third-order nonlinear optical susceptibility in RE doped tellurite glasses made them fascinating for diverse applications in photonics [1-6]. These glasses are not only resistant to atmospheric moisture but also allow the incorporation of high rare-earth ions concentration into the matrix [7]. The understanding on microscopic mechanism of their low phonon cutoff, notable nonlinear optical response and high quantum efficiency provided further impetus towards industrial applications and fundamental interests in academia [8, 9]. Moreover, the assimilation of RE ions stabilizes the metastable crystalline phase useful for assorted functions [10]. Recently, the RE ions based glasses attracted renewed interests due to their technological utilities [11]. Lead glasses have several daily life applications due to their special properties such as ease formation ability, elevated refractive index, reduced working temperature and low viscosity. It is the large refractive index and low loss in phonon energy permit lead-tellurite glass to improve their fluorescence emission compare to other oxide hosts. Despite much research the mechanism on RE concentration dependent absorption modification are not analyzed using J-O theory.

*Corresponding author: mrahim057@gmail.com

Enhanced optical properties of RE doped glasses for sundry optical applications are the current challenge in materials science and technology. Among the RE ions, Er^{3+} is the most widely studied and optically efficient one. Conversely, the optical properties of Er^{3+} are interesting due to their use in infrared lasers operating at eye-safe wavelength and in the fabrication of optical amplifiers [12]. However, the small absorption and emission cross sections of Er^{3+} needs considerable enhancement [13]. Recently, the energy transfer from samarium to erbium ions in co-doped zinc phosphate glass is suggested towards such enhancement [14]. Furthermore, an increase in the concentration of RE also causes UV shift in the optical absorption bands and increases the photoluminescence intensities [15].

The J-O intensity parameters render significant information regarding local structure and bonding in the vicinity of rare-earth ions. The parameter Ω_2 is related with the symmetry of the glass hosts while Ω_6 is a measure of the covalency in the network [16, 17]. These parameters can have considerable influence on the stimulated emission cross-section, fluorescence decay and hence on the quantum efficiency of the glassy material [18]. They are highly sensitive to the accuracy of the absorption measurements and the transitions used in the fitting [19]. Lately, an increase in Ω_2 and Ω_6 parameters in addition to the enhancement of green and red emissions in erbium doped zinc tellurite glasses in the presence gold nanoparticles is demonstrated [20].

We report the absorption characteristics and the variation in J-O intensity parameters of Er^{3+} doped lead-tellurite glasses. The radiative transition rates and oscillator strengths are determined to relate their dependence on RE concentrations. Results on absorption features are analyzed and compared.

2. Experimental

Series of four glass samples of the form $(80\text{-}x)TeO_2\text{-}15PbO\text{-}5PbCl_2\text{-}xEr_2O_3$ with $0.5 \leq x \leq 1.5$ mol% are prepared using melt-quenching technique. Analytical grade powdered TeO_2, PbO, $PbCl_2$ and Er_2O_3 of 99.99% purity are used as starting raw materials and thoroughly mixed before placing inside the furnace at 950 ^oC allowed for complete melting. The melt is then poured onto a steel mold and annealed at 250 ^oC for 3 hours to reduce the mechanical stress and avoiding embrittlement. The melt is cooled down to room temperature. Finally, the samples are cut and polished for the optical measurements. X-ray Diffraction (XRD) analysis is performed on Siemens Diffractometer D5000 using CuK_α radiations (λ=1.54 Å) at 40 kV and 100 mA, with scanning angle 2θ ranges between 10-80° to verify the amorphous nature of all glass samples. Glass densities are measured by Archimedes method via analytical balance with specific density (Precisa XT 220 A) using toluene as an immersion liquid. The room temperature absorption spectra in the range of 400-1600 nm are recorded by using Shimadzu UV-3101PC (Kyoto, Japan) scanning spectrophotometer.

3. Results and Discussion

Figure 1 shows the typical XRD pattern for glass with 1.0 mol% of Er_2O_3. The complete absence of any sharp peaks in the spectra confirms the amorphous nature of the prepared glass [21].

The UV-Vis-NIR absorption spectra for all the samples as shown in Figure 2 display seven prominent peaks centered at 490, 526, 551, 652, 800, 982 and 1520 nm originating from the ground state ($^4I_{15/2}$) to excited states ($^4F_{7/2}$, $^2H_{11/2}$, $^4S_{3/2,}$ $^4F_{9/2}$, $^4I_{9/2}$, $^4I_{11/2}$ and $^4I_{13/2}$) transitions. The occurrence of all these peaks are in agreement with other findings [16, 17, 22]. Absorbance peak for $^4I_{15/2} \rightarrow {}^2H_{11/2}$ transition shows the highest intensity among all glass samples. Furthermore, an increase in Er^{3+} ion concentration enhances the absorbance intensity accompanied by peak shift towards shorter wavelength which is ascribed to the structural rearrangement in the glass [20].

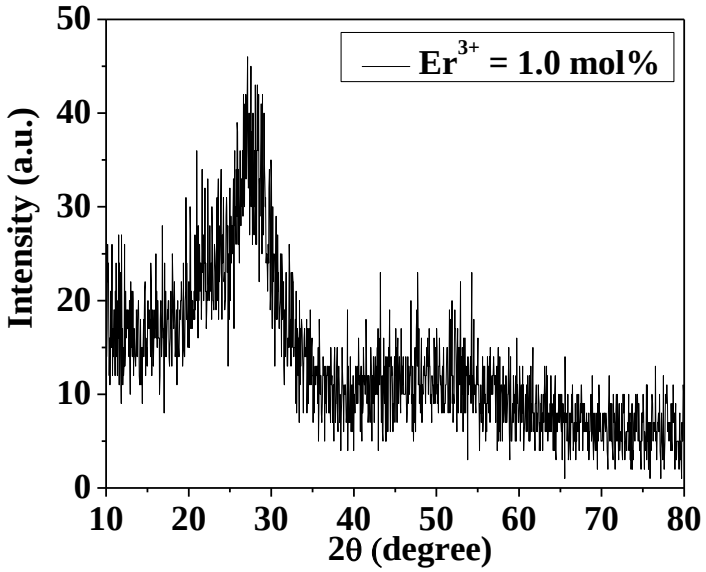

Fig. 1: X-ray diffraction patterns for glass with 1.0 mol% of Er_2O_3.

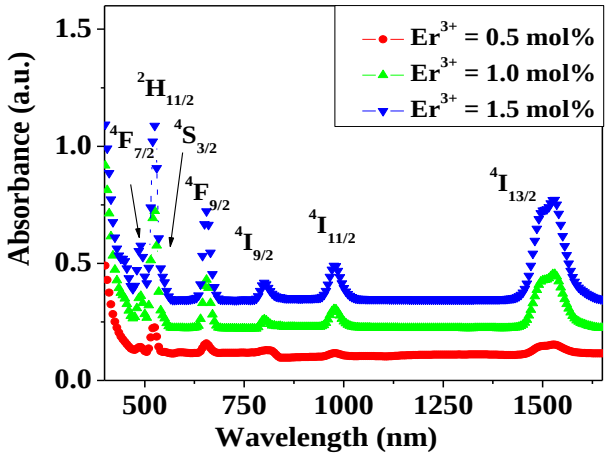

Fig. 2: Absorption spectra of glasses for varying concentration of Er_2O_3.

Detailed studies on Ω_λ are important for investigating the local structure, bonding in the vicinity and transition properties of RE ions. Following Xy et al. [17] the experimental oscillator strengths (f_{exp}) for different transitions are obtained from the absorption spectrum using the relation,

$$f_{exp} = 4.318\times10^{-9}\int \alpha(\nu)d\nu \qquad (1)$$

where α is the molar extinction coefficient at energy ν (cm^{-1}). The calculated oscillator strength (f_{cal}) determined by the isolation of both electric-dipole and magnetic-dipole contribution from f_{exp} yields,

$$f_{cal} = \left[\frac{8\pi^2 mcv}{3h(2J+1)}\right]\left[\frac{(n^2+2)^2}{9n}\right] \times \sum_{\lambda=2,4,6} \Omega_\lambda \left(\Psi J \left\| U^\lambda \right\| \Psi' J'\right)^2 \qquad (2)$$

where n is the refractive index, J is the total angular momentum of the ground state, Ω_λ are the J-O intensity parameters used to characterize the metal-ligand band in the host matrix and $\left\| U^\lambda \right\|^2$ is the square reduced matrix elements of the unit tensor operator [23-26]. The quality of the fitting of calculated oscillator strengths to the experimental one is expressed by the root-mean-square (rms) value which is 10^{-6}.

The values of f_{cal} and f_{exp} are listed in Table 1. The strong dependence of the oscillator strengths on Er_2O_3 contents implies that the non-symmetric component of the electric field acting on the Er^{3+} lead-tellurite glasses is relatively high. The oscillator strength provides indirect information on the symmetry and bonding of RE ion within the matrix. The smaller oscillator strengths indicate higher symmetry around RE ion, whereas the larger oscillator strengths promise strong covalent nature between ligands. The hypersensitive transition being very sensitive to small changes in environment around lanthanide ions obey the selection rules, $|\Delta J| \leq 2$, $|\Delta L| \leq 2$ and $\Delta S = 0$. The radiative transitions within $4f^n$ configuration of rare-earth ion are analyzed using J-O parameters [23, 24]. The J-O parameters are calculated from the electric dipole contributions of the experimental oscillator strength using the least square fitting approach [17] where the matrix elements are employed [23, 24, 27, 26].

Table 1: The Er_2O_3 concentration dependent experimental and calculated oscillator strengths.

Transition	**0.5 mol%**		**1.0 mol%**		**1.5 mol%**	
	f_{exp}	f_{cal}	f_{exp}	f_{cal}	f_{exp}	f_{cal}
$^4I_{13/2} \rightarrow {}^4I_{15/2}$	1.972	3.317	3.639	3.630	4.887	1.684
$^4I_{11/2} \rightarrow {}^4I_{15/2}$	0.554	1.495	1.156	1.589	4.716	0.745
$^4I_{9/2} \rightarrow {}^4I_{15/2}$	1.125	0.784	0.727	0.854	0.875	0.545
$^4F_{9/2} \rightarrow {}^4I_{15/2}$	3.029	5.038	5.214	5.513	3.668	3.068
$^4S_{3/2} {}^4 \rightarrow I_{15/2}$	0.180	1.196	0.014	1.309	0.061	0.569
$^2H_{11/2} \rightarrow {}^4I_{15/2}$	9.474	13.518	13.516	11.950	96.056	9.464
$^4F_{7/2} \rightarrow {}^4I_{15/2}$	1.111	5.075	3.527	5.585	5.727	2.692
rms ($x10^{-6}$)						

The estimation of Ω_λ requires density (ρ) and refractive index (n). Density is calculated by using Archimedes formula expressed as,

$$\rho = \frac{W_a}{W_a - W_l}(\rho_l - \rho_a) + \rho_a \qquad (3)$$

Following Dimitrov and Sakka [28] the refractive index yields,

$$\frac{n^2-1}{n^2+2} = 1 - \sqrt{\frac{E_g}{20}} \qquad (4)$$

The optical band gap (E_g) is extracted from the UV absorption edge using Davis Mott equation [29],

$$\alpha(\omega) = \frac{B}{\hbar\omega}(\hbar\omega - E_g)^n \quad (5)$$

where B is a constant, ħω is the photon energy, α is the absorption coefficients and ω is the frequency. Table 2 summarizes the density, refractive index and J-O parameters for all glass samples with different Er^{3+} contents. Interestingly, the glass density (5.65 to 5.72 $g.cm^{-3}$) and refractive index (2.37 to 2.42) both show steady increment with the increase of erbium ions concentration. This increase is attributed to the creation more of non-bridging oxygen ion.

Table 2 Density, refractive index and Judd-Ofelt parameters Ω_λ (x 10^{-20} cm^2) for glass.

Er_2O_3 (mol%)	Density (gcm^{-3})	Refractive index	Ω_2	Ω_4	Ω_6
0.5	5.65	2.37	2.89	1.32	0.83
1.0	5.76	2.41	3.94	1.81	1.65
1.5	5.72	2.42	3.23	1.96	1.82

The variation of RE concentration dependent J-O intensity parameters is illustrated in Figure 3. The value of Ω_2 is related to the symmetry of the glass hosts while Ω_6 decreases with increases of the covalence nature of the Er-O bond [6]. The values of Ω_4 and Ω_6 are in conformity with report [16, 17] while the value of Ω_2 are observed to be slightly lower [30]. The trend for the Ω parameters in the glass system follows $\Omega_2 > \Omega_4 > \Omega_6$. The value of Ω_2 signifying the dependence of covalency between the rare earth ions and ligand anions clearly reflects the presence of asymmetry of the local environment in the proximity of RE ion site. The characteristic feature of Ω_2 parameter is related to asymmetry of coordinate structure, bonding nature and polarizability of the ligand ions or molecule and is sensitive to the local environment of the RE ions. The higher value of Ω_2 representing less ionic nature of the chemical bond with the ligands is responsible for the increase in the covalent character [31, 32]. The smaller value of Ω_4 and larger Ω_6 are favorable for the luminescence transition.

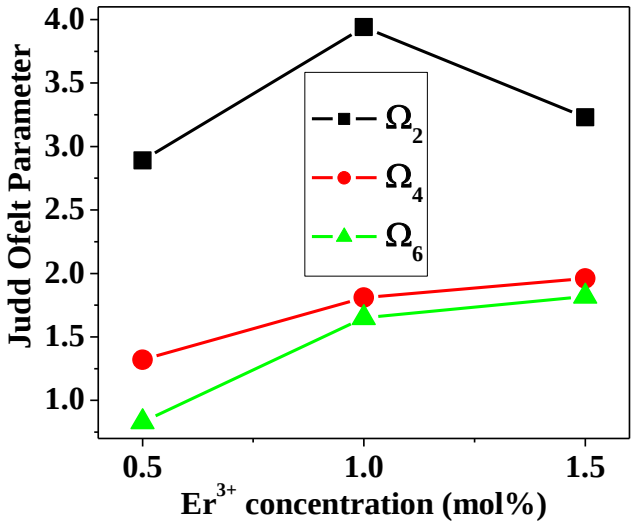

Fig. 3 The Er_2O_3 concentration dependent variation of J-O parameters Ω_λ (x 10^{-20} cm^2) for all samples.

The total spontaneous transition probability (A) contributed from the electric dipole (A_{ed}) and magnetic dipole (A_{md}) transition probability are calculated from J-O parameters [17]. The fluorescence branching ratio (β) of transitions is calculated using $\beta = A / \sum A$ and the total radiative lifetime (τ_{rad}) yields $\tau_{rad} = 1/A$. The spontaneous transition probabilities and the branching ratio are summarized in Table 3. The total spontaneous-radiative transition rates for $^4I_{13/2}$ obtained by us is much higher than the reported one [16, 17]. The large value of branching ratio (~90%) for $^4I_{9/2} \rightarrow {}^4I_{15/2}$ and $^4S_{3/2}{}^4 \rightarrow I_{15/2}$ transitions suggests that the green and red emissions in these glasses are achievable. The highest value of τ_{rad} is observed to be 1.02 ms for the glass with 0.5 mol% of Er_2O_3.

Table 3: The Er_2O_3 concentration dependent spontaneous transition probabilities, branching ratios and radiative lifetimes.

Transition	**Glass**					
	0.5 mol%		**1.0 mol%**		**1.5 mol%**	
	A	**β**	**A**	**β**	**A**	**β**
$^4I_{13/2} \rightarrow {}^4I_{15/2}$	393.20	100.00	680.41	100.00	734.80	100.00
$^4I_{11/2} \rightarrow {}^4I_{15/2}$	344.32	44.13	502.83	54.70	547.82	54.16
$^4I_{9/2} \rightarrow {}^4I_{15/2}$	7.03	97.70	6.92	98.74	7.25	98.75
$^4F_{9/2} \rightarrow {}^4I_{15/2}$	198.21	34.35	183.24	56.08	199.33	55.72
$^4S_{3/2} \rightarrow {}^4I_{15/2}$	33.06	96.55	36.48	97.76	38.70	97.34
	τ_{rad} = 1.02		**τ_{rad} = 0.71**		**τ_{rad} = 0.65**	

4. Conclusions

A series lead tellurite glasses with varying concentration of Er_2O_3 dopants are synthesized using conventional melt quenching technique. The amorphous nature of synthesized glasses is confirmed by XRD. The increase in refractive index and density with RE ions concentration is attributed to the alteration in the glass network structures. The UV-Vis-NIR spectra exhibit seven prominent peaks and the absorbance strongly depend on Er^{3+} contents. The J-O parameters employed to calculate the radiative parameters such as transition probability and branching ratio display significant improvement with the increase of RE contents. The higher oscillator strengths indicate the lower site symmetry around the Er^{3+} ion in the prepared glasses. The magnitudes of the J-O intensity parameters following the trend $\Omega_2 > \Omega_4 > \Omega_6$ demonstrates a significant increase in spectroscopic quality factors. The value of branching ratio as much as 90% is accomplished for $^4I_{9/2} \rightarrow {}^4I_{15/2}$ and $^4S_{3/2}{}^4 \rightarrow I_{15/2}$ transitions. The highest value of τ_{rad} is observed to be 1.02 ms for the glass with 0.5 mol% of Er_2O_3. The tenability of absorbance characteristics by altering Er_2O_3 contents is established. The excellent features of the results suggest that these glasses are potential candidates for diverse photonic applications.

Acknowledgements

The authors gratefully acknowledge the financial support from Malaysian Ministry of Higher Education, Malaysia and Universiti Teknologi Malaysia via grants of Vot: 4F083, 05H36 and 4L032.

References

[1] A.K. Singh, S. B. Rai, Laser and Spectroscopy Laboratory (2007).
[2] J.C. Sabadel, P. Armand, D. Cachau-Herreillat, P. Baldeck, O. Doclot, A. Ibanez,

E. Philippot, Journal of Solid State Chemistry. **132**, 411 (1997).
[3] J.S. Wang, E.M. Vogel, E. Snitzer, J. Non-Cryst. Solids. **178**, 109 (1994).
[4] R.K. Verma, K. Kumar, and S.B. Rai, Spec. Acta Part A **74**, 1052 (2004).
[5] V.R. Kumar, N. Veeraiah, J. Mat. Sci. Let. **16**, 1816 (1997).
[6] V.V. Ravi Kumar, Bhatnagar, K. Anil, R. Jagannathan (2001).
[7] Y. Nageno, H. Takeke, and H. Morinaga, J. Amor. Cer. Soc. **76**, 3081 (1993).
[8] P.N. Prasad, Nanophotonics, in John Wiley and Sons, Inc., New York. 2004.
[9] R.A.H. El-Mallawany (2002).
[10] K. Hirano, Y. Benino, T. Komatsu, J. Phys. Chem. of Sol. **62**, 2075 (2001).
[11] N. Ghoneimo, Indian J. Phys. **87**, 39 (2013).
[12] Y. K. Sharma, S. S. L. Surana, R. K. Singh, R. P. Dubedi, Opt. Mat., **29**, 598 (2007).
[13] G.N. Van Den Hoven, J.A. Van Der Elsken, A. Polman, C. Van Dam, W. M. Van Uffelen M.K. Smit, Appl. Opt. **36**, 3338 (1997).
[14] B.C. Joshi, B. Khulbey, D. Upreti and C.C. Dhaundiyal, Indian J. Phys., **4**, 405 (2010).
[15] P.S.R. Naik, M.K. Kumar, Y.N. Babu, A.S. Kumar, Indian J. Phys, **87**, 757 (2013).
[16] R.Rolli, M. Montagna, S. Chaussedent, A. Monteil, V.K Tikhomirov, M. Ferrari, Opt. Mat.. **21**, 743 (2003).
[17] S. Xy, Z.Yang, G. Wang, S. Dai, J. Zhang, L. Hu, Z. Jiang, J. of All. and Comp. **377**, 253 (2004).
[18] K. Ouannes, M.T. Soltani, M. Poulain, G. Boulon, G. Alombert-Goget, Y. Guyot, A. Pillonnet, K. Lebbou, J. of All. and Comp. (2014).
[19] P. Babu, H.J. Seo, C.R. Kesavulu, K.H. Jang, C.K. Jayasankar, J. of Lum. **129**, 444 (2009).
[20] A. Awang, S.K. Ghoshal, M.R. Sahar, M. Reza Dousti, R.J. Amjad, F. Nawaz, Curr. App. Phy. **13**, 1813 (2013).
[21] N. A. Zarifah, M. K. Halimah, M. Hashim, B. Z. Azmi, W.M. Daud, Chal. Lett., 565 (2010).
[22] S. Samah, A. Kumar, Indian J. Phys. **84**, 1211 (2010).
[23] B.R. Judd, Phys. Rev. **3**, 750 (1962).
[24] G. S. Ofelt, The Journal of Chemical Physics. **37**, 511 (1962).
[25] J.A. Capobianco, G. Prevost, P.P. Proulux, P. Kabro and M. Bettinelli, Opt. Mat. **6**, 175 (1996).
[26] R.D. Peacock, Struct. Bonding. **22**, 83 (1957).
[27] R. Reisfield, Struct Bonding. **22**, 123 (1975).
[28] V. Dimitrov, S. Sakka, J. App. Phy. **79**, 1736 (1996).
[29] M. Naser Ahmed, Z. Sauli, U. Hashim, Y. Al-Douri, Int. J. Nanoelectronics and Mat. **2**, 189 (2009).
[30] J.A. Capobianco, G. Prevost, P.P. Proulxa, P. Kabroa and M. Bettinellib, Opt. Mat. **6**, 175 (1996).
[31] C.K. Jorgensen, R. Reisfield, J. Less-Common Met., 107 (1983).
[32] P. Subbalakshmi, N. Veeraiah, J Phys. and Chem. Sol., **64**, 1027 (2003).